

Experimental and Theoretical Studies of the Site Exchanges in $\text{Rh}_4(\text{CO})_{12}$ and $\text{IrRh}_3(\text{CO})_{12}$

Katya Besançon, Gábor Laurency, Tito Lumini, and Raymond Roulet*

Institut de Chimie Minérale et Analytique de l'Université, BCH, CH-1015 Lausanne (Switzerland)

Raf Bruyndonckx and Claude Daul

Institut de Chimie Inorganique et Analytique de l'Université, Péroilles, CH-1700 Fribourg (Switzerland)

Received April 13, 1998

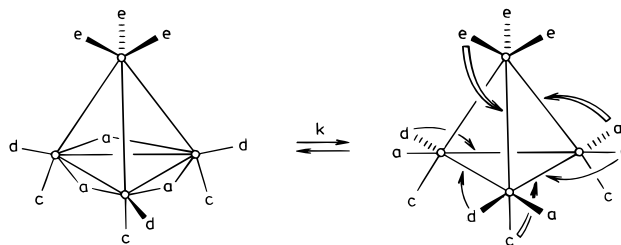
As observed by variable temperature and pressure ^{13}C NMR, the intramolecular scrambling of carbonyl ligands in $\text{Rh}_4(\text{CO})_{12}$ and $\text{IrRh}_3(\text{CO})_{12}$ is due to a merry-go-round process ($3 \mu_2\text{-CO} \leftrightarrow 3 \eta^1\text{-CO}$) about any triangular face of the metal tetrahedron. Both cluster compounds have a negative activation volume on going from the bridged ground-state structure of C_{3v} symmetry to an unbridged transition state, suggesting that bridged M–M distances are longer than unbridged M–M distances. Site exchange is faster in $\text{Rh}_4(\text{CO})_{12}$ than in $\text{IrRh}_3(\text{CO})_{12}$ where the apical position is occupied by an iridium atom. Density functional calculations on the bridged and unbridged forms of both cluster compounds have been made at two levels of approximation (LDA and GGA) including relativistic effects for Ir and Rh. LDA reproduces best the experimental distances and shows that opening bridges shortens the M–M bonds. The difference in volume of the bridged and unbridged forms of $\text{Rh}_4(\text{CO})_{12}$, as calculated from Connolly surfaces, agrees fairly well with the experimental activation volume. Calculations at the GGA level give the correct trends in energies. ELF maps and overlap population analysis indicate that iridium is more electropositive than rhodium, as suggested by the experimental results.

Introduction

The bulk of the studies on the fluxional behavior of clusters compounds have dealt with the migration of carbon monoxide over tri- and tetrametallic carbonyl clusters^{1–4} and have led to two theories for the mechanism of carbonyl scrambling.^{5–7} The first proposal was made by F. A. Cotton in 1966⁵ and involves bridge opening and closing of the carbonyl ligands to move them around the cluster in concerted steps. This is the so-called merry-go-round, whose features were essentially deduced from the comparison of the ^{13}C NMR spectra of $\text{Rh}_4(\text{CO})_{12}$ in the slow and fast exchange domains. The ground-state geometry of $\text{Rh}_4(\text{CO})_{12}$ in solution has C_{3v} symmetry,^{8,9} as in the solid.^{10–12} In the fast exchange domain, CO scrambling is complete and intramolecular, as a single quintet was observed due to coupling to four equivalent ^{103}Rh nuclei. This led to

- (1) Johnson, B. F. G.; Rodgers, A. In *The Chemistry of Metal Cluster Complexes*; Schriver, D. F., Kaesz, H. D., Adams, R. D., Eds.; VCH: New York, 1990.
- (2) Aime, S.; Dastru, W.; Gobetto, R.; Krause, J.; Violano, L. *Inorg. Chim. Acta* **1995**, 235, 757.
- (3) Adams, H.; Chen, X.; Mann, B. E. *J. Chem. Soc., Dalton Trans.* **1996**, 2159.
- (4) Roulet, R. In *The Synergy Between Dynamics and Reactivity at Clusters and Surfaces*; Farrugia, L. J., Ed.; Kluwer: The Netherlands, 1995.
- (5) Cotton, F. A. *Inorg. Chem.* **1966**, 5, 1083.
- (6) Johnson, B. F. G.; Benfield, R. E. *J. Chem. Soc., Dalton Trans.* **1978**, 1554.
- (7) Johnson, B. F. G.; Roberts, Y. V. *Inorg. Chim. Acta* **1993**, 205, 175.
- (8) Cotton, F. A.; Kracynski, L.; Shapiro, B. L.; Johnson, L. F. *J. Am. Chem. Soc.* **1972**, 94, 6191.
- (9) Evans, J.; Johnson, B. F. G.; Lewis, J.; Norton, J. R. *J. Chem. Soc., Chem. Commun.* **1973**, 807.
- (10) Wei, C. H.; Wilkes, G. R.; Dahl, L. F. *J. Am. Chem. Soc.* **1967**, 89, 4792.
- (11) Wei, C. H. *Inorg. Chem.* **1969**, 8, 2384.
- (12) Carré, F. H.; Cotton, F. A.; Frenz, B. A. *Inorg. Chem.* **1976**, 15, 380.

Scheme 1



the proposal of a merry-go-round of six CO's about any one of the triangular faces of an unbridged transition state (Scheme 1).

Three open questions are addressed in the present report: (i) Is the unbridged species a good representation of the transition state? (ii) Does the ligand migration take place about a rigid metal core? (iii) What is the effect of replacing Rh by Ir on the site exchange processes while keeping the symmetry of the ground-state unchanged?

Numerous studies have demonstrated the importance of including pressure as a kinetic parameter in the elucidation of inorganic reaction mechanism.^{13–17} The clusters $\text{M}_4(\text{CO})_{12}$ are suitable for variable pressure studies, as there is no charge creation or annihilation on forming the transition state. The electrostriction can therefore be neglected, and the activation volume ΔV^\ddagger can be deduced from the variable pressure NMR

- (13) Van Eldik, R., Ed. *Inorganic High-Pressure Chemistry: Kinetics and Mechanisms*; Elsevier: Amsterdam, 1986.
- (14) Van Eldik, R.; Asano, T.; le Noble, W. J. *Chem. Rev.* **1989**, 89, 549.
- (15) Merbach, A. E. *Pure Appl. Chem.* **1987**, 59, 161.
- (16) Merbach, A. E.; Akitt, J. W. *NMR: Basic Princ. Prog.* **1990**, 24, 189.
- (17) Laurency, G.; Merbach, A. E.; Moullet, B.; Roulet, R.; Hoferkamp, L.; Süß-Fink, G. *Helv. Chim. Acta* **1993**, 76, 2936.

spectra using eq 1 where k_0 is the rate constant of the site exchange process at 0.1 MPa.

$$\ln k = \ln k_0 - (\Delta V^\ddagger P/RT) \quad (1)$$

The first two questions will be answered by comparing the experimental value of ΔV^\ddagger to the difference in volume between the ground state and the supposedly unbridged transition state, as obtained by DFT calculations on Rh₄(CO)₁₂ (C_{3v} and T_d). The third question will be answered by comparing the site exchange in Rh₄(CO)₁₂ and IrRh₃(CO)₁₂, the latter having also a ground state of C_{3v} symmetry.

Experimental Section

All operations were carried out under N₂ using standard Schlenk techniques. Solvents were purified, distilled from the appropriate drying agents, and stored under N₂. IR spectra were taken on a Perkin-Elmer FT IR 2000 spectrophotometer. Rh₄(CO)₁₂ was prepared by the literature method.¹⁸ The reference for the preparation of IrRh₃(CO)₁₂ is given in the text.

NMR Measurements. The spectra at variable pressure and temperature were recorded using a Bruker AC-200 spectrometer (4.7 T) working at 50.323 MHz. The variable temperature measurements were made between 203 and 293 K for Rh₄(CO)₁₂, and 243 and 323 K for IrRh₃(CO)₁₂. The variable pressure measurements were made up to 2000 bar using a home-built high-pressure probe, designed for a Bruker narrow-bore cryomagnet.¹⁹ A built-in platinum resistor allowed temperature measurements with an accuracy of ± 1 K. When a thermostated liquid was pumped through the bomb, the temperature was stabilized to ± 0.2 K. The spectra were obtained by using 32 K data points resulting from 17 000 to 25 000 scans accumulated over a total spectral width of 17 kHz. To improve the signal-to-noise ratio, exponential filters (line-broadening) of 5 Hz were used. ¹³C chemical shifts are referred to TMS and measured with respect to the solvent CD₂Cl₂ signal at 53.2 ppm.

The EXSY ¹³C NMR spectra were obtained in CD₂Cl₂ from NOESY experiments using TPPI.²⁰ The spectral width was 7575.7 Hz in both F1 and F2 domains, a shifted squared cosine bell was applied in both domains prior to Fourier transformation. The mixing time was 50 or 100 ms.

Calculations. The density functional (DF) calculations reported in this paper were carried out with the Amsterdam density functional (ADF) program package.^{21–25} The computational scheme is characterized by a density fitting procedure to obtain the Coulomb potential²² and by elaborate 3D numerical integration techniques for the evaluation of the Hamiltonian matrix elements, including those for the exchange correlation potential.^{23,25} Two different density functionals were used in our study: the Vosko–Wilk–Nusair parametrization of the electron gas for the local density approximation (LDA),²⁶ and the generalized gradient approximation (GGA) with the exchange part by Becke²⁷ and the functional of Perdew for correlation.²⁸

As basis sets for describing the molecular orbitals we used the uncontracted Slater-type orbitals (STO) as implemented in the ADF basis set library. For C and O a triple- ζ STO basis set, augmented with a 3d polarization function, was used, whereas for Ir and Rh this triple- ζ STO's were augmented with a p polarization function. The

electrons in the lower shells (Ir, 1s–4d; Rh, 1s–3d; C and O, 1s) were treated in the frozen core approximation. First calculations were done using a 1s–5p frozen core approximation for Ir, because the more extended 1s–4d frozen core Ir basis set has only been made available recently with ADF release 2.3. We want to warn the ADF users from using the Ir(1s–5p) basis set. We have noticed that, when applying the relativistic corrections, the basis has an erroneous behavior. The main effect is that the atom becomes too polarizable and loses too much of its density/charge. We have observed e.g. effective charges of about +2.0 on Ir, whereas we believe this should be much smaller (± 0.2). This results not only in an overestimation of the bond lengths between Ir and directly connected atoms (Rh and Ce), but also affects the Rh–Rh bonds. These latter atoms are actually calculated with a small (and even negative) charge. All these suspicious effects were removed when using the more extended Ir(1s–4d) basis set.

An important aspect for dealing with third row transition metals (Ir) is the treatment of relativistic effects in the molecular calculations. It has been demonstrated that including the scalar relativistic terms (Darwin and mass-velocity) at the so-called quasi-relativistic level is adequate for most chemical purposes.^{29,30} The way this is implemented in ADF is by evaluating scalar relativistic effects on valence electrons by means of perturbation methods.³¹ This treatment is applied on IrRh₃(CO)₁₂ as well as on Rh₄(CO)₁₂ for the sake of comparison.

To get an estimate for the activation volumes, a procedure based on the Connolly surface was used.^{32,33} From the molecular coordinates obtained with the ADF calculations, the volume of the different conformations (bridged and unbridged) was calculated as the one being enclosed by the solvent-accessible surface. This method consists of smoothening the van der Waals surface (= the union of spheres with the appropriate van der Waals radius at the atomic positions) by rolling over it with a probe with given radius and hereby overlapping the crevices and pits. This surface represents the boundary of the volume from which a probe sphere is excluded if it is not to experience van der Waals overlap with the atoms.

Results and Discussion

¹³C NMR Study of the Site Exchanges in Rh₄(CO)₁₂ and IrRh₃(CO)₁₂. The assignment of the ¹³C resonances of Rh₄(CO)₁₂ was based on the C,Rh coupling constants and corresponds to that proposed by B. T. Heaton.³⁴ Line-shape analysis of the variable temperature ¹³C NMR spectra of a sample of Rh₄(CO)₁₂ enriched in ¹³CO (ca. 30%) in CD₂Cl₂ (Figure 1) was made on the basis of the Cotton mechanism using the following exchange matrix and taking into account all the spin states of the CO ligands: $a \rightarrow ({}^1/9a, {}^4/9d, {}^2/9c, {}^2/9e)$, $d \rightarrow ({}^4/9a, {}^1/9d, {}^2/9c, {}^2/9e)$, $c \rightarrow ({}^2/9a, {}^2/9d, {}^3/9c, {}^2/9e)$, and $e \rightarrow ({}^2/9a, {}^2/9d, {}^2/9c, {}^3/9e)$. An Eyring regression of $\ln(k/T)$ vs $1/T$ gave a free enthalpy of activation of 42.8 ± 0.4 kJ mol⁻¹ at 298 K for the merry-go-round.

The variable pressure ¹³C NMR spectra of Rh₄(CO)₁₂ in CD₂Cl₂ using the same exchange matrix gave an activation volume of -6 ± 1 cm³ mol⁻¹ (Figure 2), indicating that the transition state has a smaller molar volume than the bridged ground state. Since the opening of bridges should lead to an increase in volume, the negative value of ΔV^\ddagger suggests a substantial shortening of the unbridged M–M bonds relative to the bridged ones. This suggestion will be further examined below with the help of DFT calculations. On the experimental side, there is to date no example of a Rh₄ cluster with terminal ligands only. However, a statistical study of X-ray diffraction data has shown that the differences between the mean bond lengths for un-

(18) Martinengo, S.; Chini, P.; Giordano, G. *J. Organomet. Chem.* **1971**, *27*, 389.

(19) U. Frey, L. Helm, A. E. Merbach, *High Pres. Res.* **1990**, *2*, 237.

(20) G. Bodenhausen, H. Kogler, R. R. Ernst, *J. Magn. Reson.* **1984**, *58*, 370.

(21) *ADF 2.0.3*; Theoretical Chemistry, Vrije Universiteit, Amsterdam.

(22) Baerends, E. J.; Ellis D. E.; Ros P. *Chem. Phys.* **1973**, *2*, 41.

(23) te Velde, G.; Baerends, E. J. *J. Comput. Phys.* **1992**, *99*, 84.

(24) Fonseca Guerra, C.; et al. *METECC-95* **1995**, 305.

(25) Boerrigter, P. M.; te Velde, G.; Baerends, E. J. *Int. J. Quantum Chem.* **1988**, *33*, 87.

(26) Vosko, S. H.; Wilk, L.; Nusair, M. *Can. J. Phys.* **1980**, *58*, 1200.

(27) Becke, A. D. *Phys. Rev. A* **1988**, *38*, 3098.

(28) Perdew, J. P. *Phys. Rev. B* **1986**, *33*(12), 8822.

(29) Grant, I. P. *Adv. Phys.* **1970**, *19*, 747.

(30) Ziegler, T.; et al. *J. Phys. Chem.* **1989**, *93*, 3050.

(31) Snijders, J. G.; Baerends, E. J. *Mol. Phys.* **1978**, *36*, 1789.

(32) Connolly, M. L. *J. Appl. Crystallogr.* **1983**, *16*, 548.

(33) Connolly, M. L. *J. Am. Chem. Soc.* **1985**, *107*, 1118.

(34) Heaton, B. T.; Strona, L.; Della Pergola, R.; Garlaschelli, L.; Sartorelli, U.; Sadler, I. H. *J. Chem. Soc., Dalton Trans.* **1983**, 173.

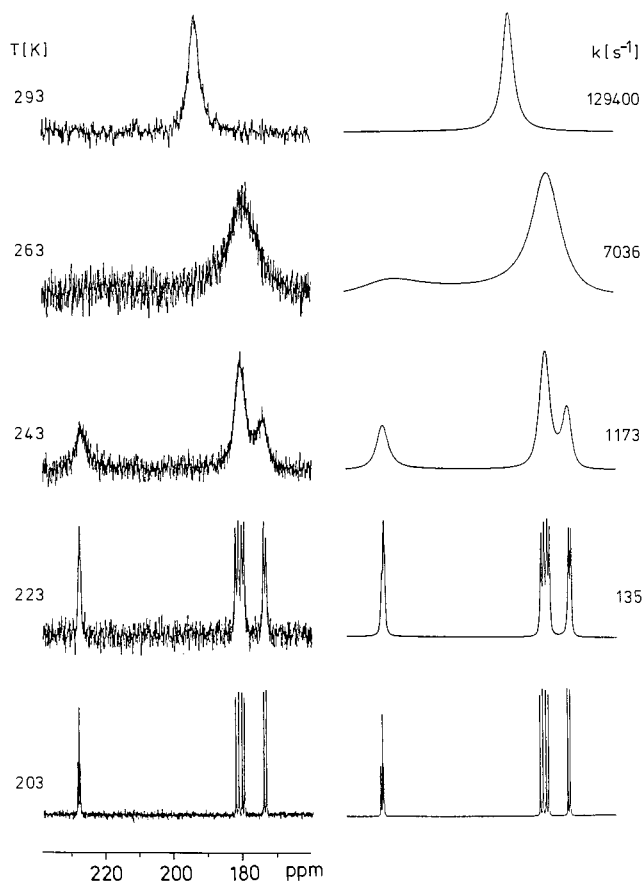


Figure 1. Measured (a) and calculated (b) ^{13}C NMR spectra of $\text{Rh}_4(\text{CO})_{12}$ in CD_2Cl_2 at different temperatures.

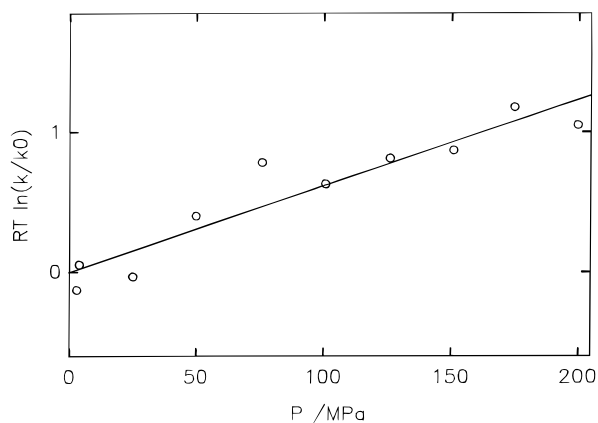


Figure 2. Effect of pressure on the rate of CO exchange in $\text{Rh}_4(\text{CO})_{12}$.

bridged and CO-bridged M–M bonds have values of -0.027 and -0.019 Å for Rh and Ir, respectively.^{35,36}

$\text{IrRh}_3(\text{CO})_{12}$ has been mentioned as a minor side product of the preparation of $\text{Ir}_2\text{Rh}_2(\text{CO})_{12}$,³⁷ but is now available in good yields by the redox co-condensation of $[\text{Rh}(\text{CO})_2(\text{THF})_x]\text{PF}_6$ and $\text{Na}_3[\text{Ir}(\text{CO})_3]$ (3:1) under CO.³⁸ Its crystals are twinned, disordered, and unsuitable for standard X-ray analysis. A solution in CH_2Cl_2 displays an IR band at 1878 cm^{-1} , indicating the presence of bridging CO's. A ^{13}C NMR spectrum of a

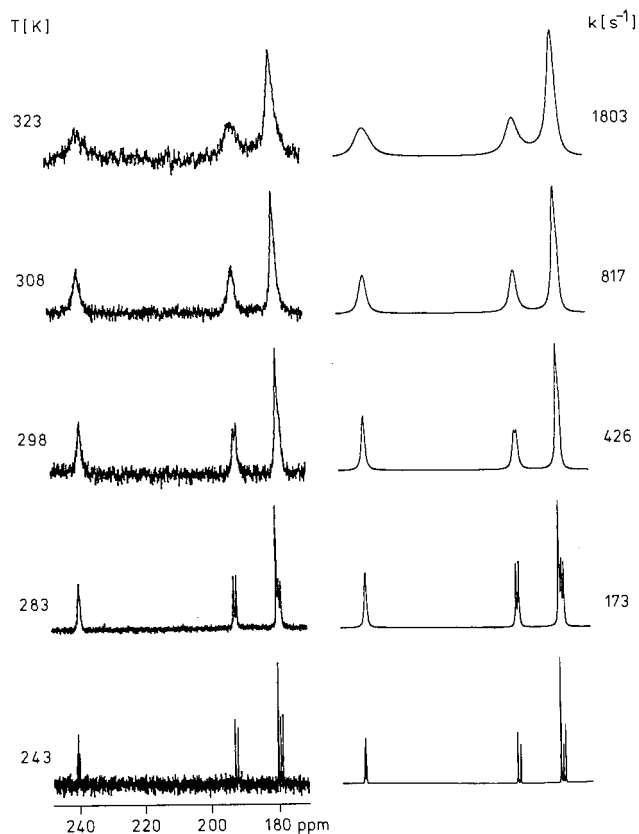


Figure 3. Measured (a) and calculated (b) ^{13}C NMR spectra of $\text{IrRh}_3(\text{CO})_{12}$ in CD_2Cl_2 at different temperatures.

sample of $\text{IrRh}_3(\text{CO})_{12}$ enriched in ^{13}C O (ca. 30%) in CD_2Cl_2 at 243 K (Figure 3) shows 4 resonances of equal intensities, indicating that the ground-state geometry has C_{3v} symmetry with the Ir-atom in apical position. The assignment of the resonances to the bridging (*a*), radial (*d*), apical (*e*), and axial (*c*) CO's was made by comparison with those of $\text{Rh}_4(\text{CO})_{12}$. The assignment of the two doublets was confirmed by a 2D-COSY spectrum, which showed a cross-peak between the singlet at 167.6 ppm (*e*) and the doublet at 166.6 ppm, due to the pseudo-trans C,C coupling between the apical and axial CO's.

A 2D-EXSY spectrum at 263 K (mixing time = 50 ms) (Figure 4) showed the following dynamic connectivities: $a \leftrightarrow (d, e, c)$, $d \leftrightarrow (a, e, c)$, $e \leftrightarrow (a, d)$, and $c \leftrightarrow (a, d)$. Integration of the cross-peaks showed them to be all of first order. Several types of exchange matrixes failed to reproduce the experimental spectra: (i) matrixes allowing spin changes during the transfer of a carbonyl ligand from one Rh atom to another; (ii) matrixes corresponding to changes of basal face with one bridging CO not exchanging, such as that used successfully for $\text{Ir}_4(\text{CO})_{10}$ -(η^2 -diars),^{39–41} and (iii) matrixes with two rate constants, one for a merry-go-round about the Rh_3 face (since the 2D-EXSY spectrum shows the connectivity $a \leftrightarrow d$), and one for a merry-go-round about an IrRh_2 face. The failure of (i) indicates that the site exchanges are intramolecular, that of (ii) and (iii) suggests that the opening of 3 bridges should occur in one step and that this step is rate determining.

Effectively, line-shape analysis of the variable temperature ^{13}C NMR spectra of $\text{IrRh}_3(\text{CO})_{12}$ could be achieved with only

(35) Braga, D.; Grepioni, F. *J. Organomet. Chem.* **1987**, 336, C9.

(36) Braga, D.; Grepioni, F.; Byrne, J. J.; Calhorda, M. J. *J. Chem. Soc., Dalton Trans.* **1995**, 3287.

(37) Martinengo, S.; Chini, P.; Albano, V. G.; Cariati, F.; Salvatori, T. *J. Organomet. Chem.* **1973**, 59, 379.

(38) Besançon, K. Ph.D. Thesis, University of Lausanne, 1996.

(39) Shapley, J. R.; Stuntz, G. F.; Churchill, M. R.; Hutchinson, J. P. *J. Am. Chem. Soc.* **1979**, 101, 7425.

(40) Churchill, M. R.; Hutchinson, J. P. *Inorg. Chem.* **1980**, 19, 2765.

(41) Strawczynski, A.; Ros, R.; Roulet, R.; Grepioni, F.; Braga, D. *Helv. Chim. Acta* **1988**, 71, 1885.

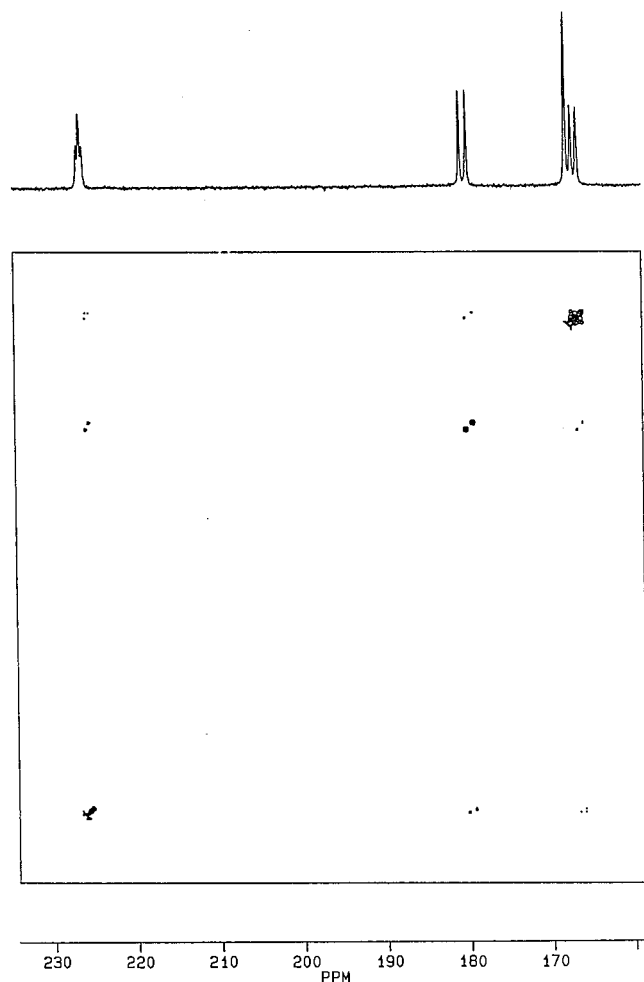


Figure 4. 2D EXSY ^{13}C NMR spectrum at 263 K (mixing time = 50 ms) of $\text{IrRh}_3(\text{CO})_{12}$ in CD_2Cl_2 .

one exchange matrix taking into account all the spin states and requiring only one rate constant k (Figure 3). This matrix corresponds to the following site exchanges: $a \leftrightarrow (1/3a, 1/3d, 1/6e, 1/6c)$, $d \leftrightarrow (1/3a, 1/3d, 1/6e, 1/6c)$, $e \leftrightarrow (1/6a, 1/6d, 2/3e)$, and $c \leftrightarrow (1/6a, 1/6d, 2/3c)$. These site exchanges are illustrated in Scheme 2.

The temperature range examined was 60 K. Above ca. 330 K, the compound started to decompose slightly and the corresponding spectra were not included in the calculation. However, a single resonance was observed in the fast exchange domain. Its frequency corresponded to the arithmetical mean of the 4 frequencies observed at low temperature, indicating complete scrambling. An Eyring regression of $\ln(k/T)$ vs $1/T$ gave a free enthalpy of activation of $57.9 \pm 0.6 \text{ kJ mol}^{-1}$ at 298 K for the merry-go-round. The variable pressure ^{13}C NMR spectra of $\text{IrRh}_3(\text{CO})_{12}$ in CD_2Cl_2 at 278 K, using the same exchange matrix as above, gave a volume of activation of $-7.7 \pm 0.6 \text{ cm}^3 \text{ mol}^{-1}$ (Figure 5), which is quite similar to that of $\text{Rh}_4(\text{CO})_{12}$.

The interpretation of the experimental results is not unequivocal. An observed negative volume of activation is not necessarily related to the formation of an unbridged transition state, when the ground state is a carbonyl bridged species and when the rate determining step of site exchange is the opening of

three CO-bridges. A counter-example was found in a NMR study of $\text{Ir}_4(\text{CO})_{11}\text{P}(\text{OPh})_3$.⁴² In solution this cluster exists as an equilibrium mixture of two isomers, one having C_s symmetry with three bridging CO's and the $\text{P}(\text{OPh})_3$ ligand in axial position (A), and one with all terminal ligands (B). Process $A \rightarrow B$ is endothermic with a reaction volume $\Delta V^\circ(A \rightarrow B)$ of $-8.3 \pm 0.2 \text{ cm}^3 \text{ mol}^{-1}$. The rate-determining step is the opening of three CO-bridges, and the activation volume has a value of $-9.4 \pm 1.1 \text{ cm}^3 \text{ mol}^{-1}$.³⁸ The negative volume of activation is related to the merry-go-round about the basal face of A, but the unbridged species is not a good representation of the transition state in this case.

Additional information on $\text{Rh}_4(\text{CO})_{12}$ (and $\text{IrRh}_3(\text{CO})_{12}$) are clearly needed, which could only come out of calculations. An extended-Hückel calculation has been performed on $\text{Rh}_4(\text{CO})_{12}$ (C_{3v} and T_d),³⁶ but an activation volume cannot be derived from it, since the geometrical parameters were a priori fixed. Therefore, a calculation was undertaken using density functional theory.

Density Functional Calculations. The aim of the present calculations consists of using theoretical pieces of information to enable an interpretation of the experimental results. Hereby it should be kept in mind that the molecular systems of interest are, given the present computer technology and for the employed theoretical method, still computationally very demanding. A complete simulation of the merry-go-round process by means of a linear transit between the bridged and unbridged conformation for instance is not feasible in an acceptable period of time. Therefore, our focus was on the differences between the optimized structures and related energetic and electronic properties of both conformations (bridged and unbridged) of the complexes $\text{Rh}_4(\text{CO})_{12}$ and $\text{IrRh}_3(\text{CO})_{12}$. The symmetry was constrained to the highest possible, i.e., T_d for $\text{Rh}_4(\text{CO})_{12}$ (unbridged) and C_{3v} for the other cases.

As the structural data from X-ray diffraction analysis is only known for $\text{Rh}_4(\text{CO})_{12}$ (bridged),¹¹ the bond lengths, as obtained from the different calculation methods, are summarized in Table 1. The numbering of the different atoms is depicted in Figure 6. Because the molecule is slightly distorted in the crystal, we averaged out the deviations in the X-ray structure to represent the idealized C_{3v} symmetry.

Concerning the metal-metal bond lengths, we observe that the LDA functional is in much better agreement with experiment than GGA. LDA including the relativistic treatment slightly underestimates the metal-metal bond length (-0.032 and -0.058 \AA), whereas LDA without relativistic correction is a bit over the experimental result ($+0.028$ and $+0.044 \text{ \AA}$). GGA on the other hand yields in both cases too long bond lengths, with a difference ranging from $+0.18$ to $+0.28 \text{ \AA}$. For the other bond lengths, the calculated results are, except for one, close to the measured values and fall within the experimental precision range. Only for the bridging carbonyl groups we obtain, with all four methods of calculation, a slightly longer $\text{Rh}_b\text{-C}_a$ bond and on the other hand a prediction of the $\text{C}_a\text{-O}_a$ bond length that is too short. But here one should remember that the crystal structure is distorted and that, for instance for the $\text{C}_a\text{-O}_a$ bond length, values ranging from 0.96 to 1.52 \AA are reported.⁴³

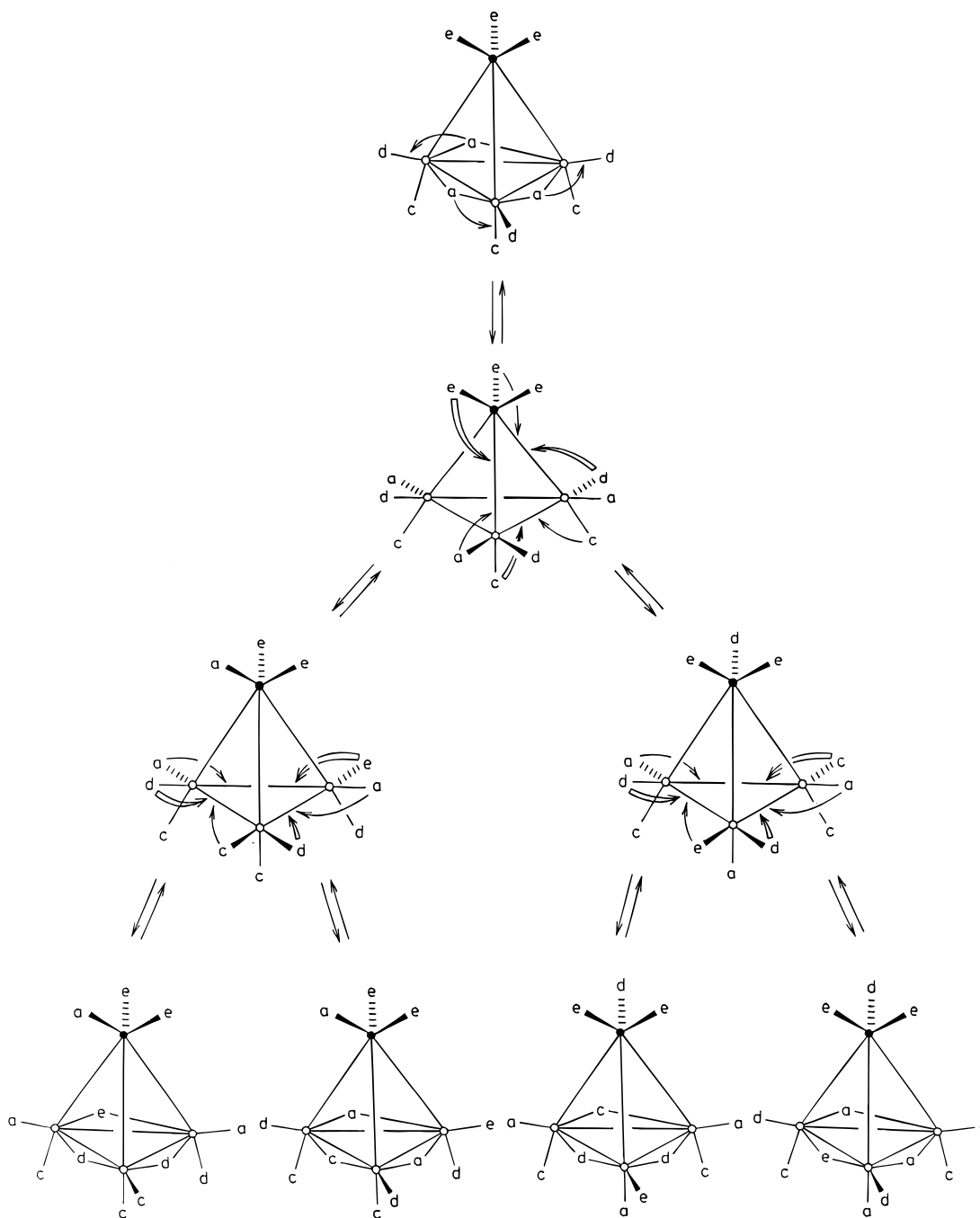
From the calculated geometrical parameters, the following trends can be deduced:

(i) The incorporation of the gradient correction into the density functional gives rise to an elongation of the bond lengths. This is a general trend within DF theory due to an erroneous description of the tail density in LDA. This leads to an overestimation of the binding energy and hence to a prediction

(42) Besançon, K.; Laurency, G.; Lumini, T.; Roulet, R.; Gervasio, G. *Helv. Chim. Acta* **1993**, *76*, 2926.

(43) Ziegler, T. *Chem. Rev.* **1991**, *91*, 651 and refs therein.

Scheme 2



of the bond lengths that is too short. Bray *et al.*⁴⁴ have shown that by including the GGA correction (the same as we used), the M–CO distances in organometallic compounds are corrected with respect to a LDA calculation and approach closely the experimental values. Nevertheless, we observe that, regarding the Rh–Rh bonds, GGA completely fails and LDA performs much better.

(ii) Applying the relativistic correction results in a contraction of the Rh–Rh and Rh–C bonds relative to nonrelativistic calculations (with one exception: Rh_a–Rh_b using GGA), but a

slight elongation of the C–O bonds is observed. This result also correlates with previous studies, which demonstrate the same effect on M–C (M = Cr, Mo, W) and C–O bond lengths.^{45–47}

These results led us to conclude that, for further calculations on the unbridged Rh₄(CO)₁₂ conformer and for IrRh₃(CO)₁₂, the best method for optimizing the structure is LDA with incorporation of relativistic correction. The values obtained from these calculations are reported in Table 2.

Looking at the different bond lengths between the two conformations (bridged–unbridged) of each cluster, we notice a shortening of the metal–metal bonds going from the bridged to the unbridged form. This change ranges from 0.005 to 0.085 Å. The same trend was observed by Braga *et al.*,^{35,36} as mentioned above. As the four metals do form the tetrahedral

(44) Bray, M. R.; Deeth, R. J.; Paget, V. J.; Sheen, P. D. *Int J. Quantum Chem.* **1996**, *61*, 85.

(45) Li, J.; Schreckenbach, G.; Ziegler, T. *J. Phys. Chem.* **1994**, *98*, 4838.

(46) Li, J.; Schreckenbach, G.; Ziegler, T. *J. Am. Chem. Soc.* **1995**, *117*, 486.

(47) Becke, A. D.; Edgecombe, K. E. *J. Chem. Phys.* **1990**, *92*, 5397.

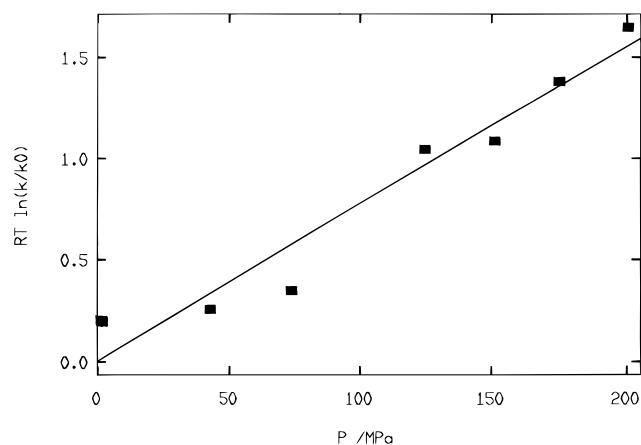


Figure 5. Effect of pressure on the rate of CO exchange in IrRh₃(CO)₁₂.

Table 1. Comparison of Experimental and Calculated Structural Parameters of Rh₄(CO)₁₂ (Bridged)

distances (Å)	exp ^a	LDA		GGA	
		relativ.	nonrelativ.	relativ.	nonrelativ.
Rh _a –Rh _b	2.715(8)	2.683	2.743	2.996	2.972
Rh _b –Rh _b '	2.749(7)	2.695	2.793	2.922	2.984
Rh _a –C _e	1.98(6)	1.905	1.939	1.933	1.967
C _e –O _e	1.16(7)	1.147	1.145	1.155	1.154
Rh _b –C _d	1.88(6)	1.879	1.902	1.906	1.936
Rh _b –C _c	2.01(7)	1.890	1.911	1.913	1.945
C _d –O _d	1.16(7)	1.147	1.145	1.155	1.154
C _c –O _c	1.11(8)	1.147	1.145	1.155	1.154
Rh _b –C _a	1.99(7)	2.065	2.092	2.120	2.150
C _a –O _a	1.36(8)	1.166	1.163	1.172	1.170

^a Reference 11.

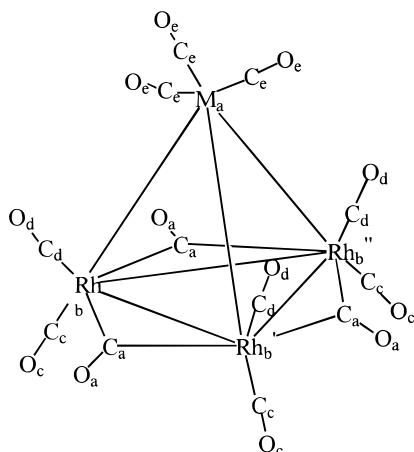


Figure 6. Numbering scheme for Rh₄(CO)₁₂ and IrRh₃(CO)₁₂.

backbone of these molecules, this gives an indication for the observed negative activation volume. Considering the M–C and C–O bond distances, we observe that there is hardly any change in their length for the terminal CO's going from the bridged to the open structure. On the contrary, for the bridging carbonyls both Rh–C and C–O bonds are elongated with respect to the terminal CO's, and this to the same extent in both molecules. The reason for this is that, due to the bridging interaction, the overlap between Rh and C is reduced which leads to the observed elongation. In fact, this phenomenon is nicely illustrated in Figures 7 and 8 which do represent the electron localization function (ELF)⁴⁸ contour map (color-coded map) of both the open and the bridged structures of Rh₄(CO)₁₂ and IrRh₃(CO)₁₂, respectively. The consideration of ELF

Table 2. Optimized Structural Parameters of Rh₄(CO)₁₂ and IrRh₃(CO)₁₂ Using LDA + Relativistic Corrections

distances (Å)	Rh ₄ (CO) ₁₂		IrRh ₃ (CO) ₁₂	
	C _{3v} (bridged)	T _d (open)	C _{3v} (bridged)	C _{3v} (open)
M _a –Rh _b	2.683	2.610	2.572	2.564
Rh _b –Rh _b '	2.695	2.610	2.672	2.617
M _a –C _e	1.905	1.897	1.901	1.889
C _e –O _e	1.147	1.149	1.146	1.149
Rh _b –C _d	1.879	1.897	1.880	1.892
Rh _b –C _c	1.890	1.897	1.900	1.904
C _d –O _d	1.147	1.149	1.146	1.148
C _c –O _c	1.147	1.149	1.149	1.150
Rh _b –C _a	2.065	/(=Rh _b –C _d)	2.063	/(=Rh _b –C _d)
C _a –O _a	1.166	/(=C _d –O _d)	1.167	/(=C _d –O _d)

provides a useful tool for the topological analysis of localization/delocalization of chemical bonds.^{48,49} These figures do represent a ELF map in the plane containing the three basal Rh atoms, for (a) the open and (b) the bridged conformations of both complexes. Inspection of this figure clearly demonstrates a delocalization of a bond over three centers Rh–(CO)–Rh in case (b) and a localization of the bond between two Rh atoms in case (a), thus leading to the observed bond length shortening in the latter case.

Whereas the LDA functional gives good results for the structural parameters, one has to apply the GGA functional to obtain accurate energy values. The obtained results of these calculations are reported in Table 3. We have found that for both cases the bridged conformation is the most stable structure. For Rh₄(CO)₁₂ the energy difference is –55 kJ mol^{–1}, and for IrRh₃(CO)₁₂ we obtained –93.5 kJ mol^{–1}. These results are not directly comparable with the experimental free enthalpies of activation (vide supra) because our method of calculation does treat the molecules in gas phase. Nevertheless these values confirm generally the observed ground state and the faster rearrangement of Rh₄(CO)₁₂ than of IrRh₃(CO)₁₂.

Table 4 lists the volumes of the different systems as obtained with the procedure described above. The geometries resulting from the LDA calculations are used. The volumes are calculated with different values for the probe radius (1.8–2.2 Å). This is done to simulate the difference in the approach of a nonsymmetrical solvent as CH₂Cl₂ or CD₂Cl₂. One can imagine that if CH₂Cl₂ e.g. was to approach with its hydrogens to the molecule, the solvent molecule could penetrate more deeply into certain crevices than it would when approaching with the chlorides. This can be seen from the volumes for each complex with respect to the probe radius: the calculated volumes increase with increasing probe radius.

Comparison the values in Table 4 horizontally shows that the volumes of the bridged conformations are bigger than those of the open systems. This indicates thus a negative activation volume, as is also observed experimentally. The calculated values overestimate slightly this effect (compare with –6 ± 1 cm³/mol for Rh₄(CO)₁₂ and –7.7 ± 0.6 cm³/mol for IrRh₃(CO)₁₂ as mentioned above), but are in the right order of magnitude.

From the experiment it is observed that the dynamics “bridged open” is faster in the Rh₄ cluster than in IrRh₃(CO)₁₂. The calculated difference in total bonding energy between the two conformers of each complex are in agreement with this finding. It is therefore interesting to investigate this result more in details. Thus, another probe is to evaluate the overlap population between a basal Rh and C of the bridging carbonyl group.

(48) Savin, A.; Nesper, R.; Wengert, S.; Fässler, T. F. *Angew. Chem., Int. Ed. Engl.* **1997**, *36*, 1808.

(49) Fässler, T. F.; Savin A. *Chemie Uns. Zeit* **1997**, *31*, 110.

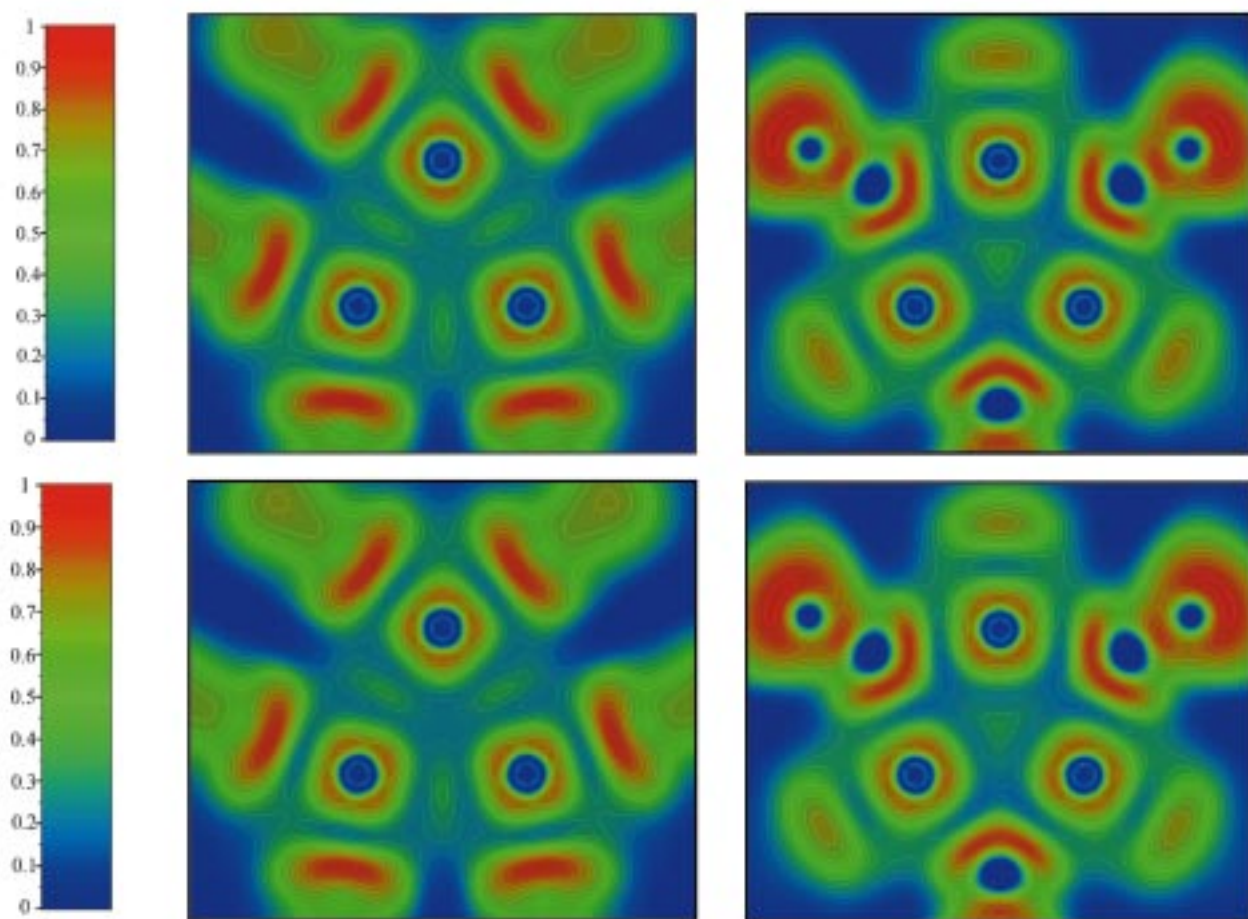


Figure 7. (top) ELF representation in the plane of the three basal Rh's for both conformations (open (a, left) and bridged (b, right)) of $\text{Rh}_4(\text{CO})_{12}$.

Figure 8. (bottom) ELF representation in the plane of the three basal Rh's for both conformations (open (a, left) and bridged (b, right)) of $\text{IrRh}_3(\text{CO})_{12}$.

Table 3. Total Bonding Energies of $\text{Rh}_4(\text{CO})_{12}$ and $\text{IrRh}_3(\text{CO})_{12}$ Using GGA + Relativistic Corrections

total bonding energy	$\text{Rh}_4(\text{CO})_{12}$		$\text{IrRh}_3(\text{CO})_{12}$	
	C_{3v} (bridged)	T_d (open)	C_{3v} (bridged)	C_{3v} (open)
kJ/mol	-20 609	-20 554	-20 904.5	-20 811
ΔE (bridged–open)		-55		-93.5

Table 4. Calculated Volumes of $\text{Rh}_4(\text{CO})_{12}$ and $\text{IrRh}_3(\text{CO})_{12}$

volume (cm^3/mol) probe radius (Å)	$\text{Rh}_4(\text{CO})_{12}$			$\text{IrRh}_3(\text{CO})_{12}$		
	C_{3v} (bridged)	T_d (open)	ΔV	C_{3v} (bridged)	C_{3v} (open)	ΔV
1.8	232	211	-21	230	221	-9
2.0	236	221	-15	233	222	-11
2.2	239	223	-16	236	223	-13

Overlap populations between atoms scale as bond strengths and hence are an indicator for the stability of an isomer. One can imagine that the stronger CO is bound, the slower the rearrangement will be. The results obtained for the atoms in the basal plane are collected in Table 5. These data always show a larger overlap population for the Rh–C bonds in $\text{IrRh}_3(\text{CO})_{12}$ than in $\text{Rh}_4(\text{CO})_{12}$, thus reflecting the higher stability of the former and the significantly more electropositive character of Ir relative to Rh. The answer to the third question raised in the

Table 5. Overlap Population of $\text{Rh}_4(\text{CO})_{12}$ and $\text{IrRh}_3(\text{CO})_{12}$

overlap population	$\text{Rh}_4(\text{CO})_{12}$		$\text{IrRh}_3(\text{CO})_{12}$	
	C_{3v} (bridged)	T_d (open)	C_{3v} (bridged)	C_{3v} (open)
$\text{Rh}_a\text{--C}_a$	0.1531	/	0.1816	/
$\text{Rh}_b\text{--C}_d$	0.2311	0.1727	0.2820	0.1907
$\text{Rh}_b\text{--C}_c$	0.2308	0.1727	0.2523	0.1907
$\text{C}_a\text{--O}_a$	0.4464	/	0.4293	/
$\text{C}_d\text{--O}_d$	0.4913	0.4838	0.4840	0.4789
$\text{C}_a\text{--O}_c$	0.4953	0.4838	0.4905	0.4789

Introduction is therefore the following: replacing Rh by Ir in the metal core of $\text{Rh}_4(\text{CO})_{12}$ results in a relative shift of electron density toward the basal face of the cluster, thus slowing the site exchange. Within each bridged conformer, both Rh–C and C–O overlap populations are larger for the terminal carbonyls. As is well-known from the metal–carbonyl bonding mode,^{50,51} back-donation into the carbonyl π^* orbital is larger for the bridging carbonyls, leading therefore to weaker Rh–C and C–O bonds. These results correlate nicely with the results described above concerning the metal–carbonyl bond lengths and the ELF contour map.

Acknowledgment. This work was supported by the Swiss National Science Foundation (Project No. 20-47'133-96 and 20-49'554-96). We thank A. Savin (Université de Paris VI) for his assistance in interpreting the ELF maps.

(50) Bauschlicher, C. W.; Bagus, P. S. *J. Chem. Phys.* **1984**, *81*, 5889.

(51) Baerends, E. J.; Rozendaal, A. *NATO ASI Ser. C* **1986**, *176*, 159.